Journal of
Applied Remote Sensing

Analyzing the spectral variability of tropical tree species using hyperspectral feature selection and leaf optical modeling

Matheus Pinheiro Ferreira
Atilio Efrain Bica Grondona
Silvia Beatriz Alves Rolim
Yosio Edemir Shimabukuro

Downloaded From: http://remotesensing.spiedigitallibrary.org/ on 12/06/2013 Terms of Use: http://spiedl.org/terms

Analyzing the spectral variability of tropical tree species using hyperspectral feature selection and leaf optical modeling

Matheus Pinheiro Ferreira,[a,b] Atilio Efrain Bica Grondona,[b] Silvia Beatriz Alves Rolim,[b] and Yosio Edemir Shimabukuro[a]
[a]National Institute for Space Research, Remote Sensing Division, Av. dos Astronautas 1758, 12227-010 São José dos Campos, SP, Brazil
mpf@dsr.inpe.br
[b]Federal University of Rio Grande do Sul, Center for Remote Sensing, Av. Bento Gonçalves, 9500 91501-970 Porto Alegre, RS, Brazil

Abstract. Hyperspectral remote sensing can provide information about species richness over large areas and may be useful for species discrimination in tropical environments. Here, we analyze the main sources of variability in leaf spectral signatures of tropical trees and examine the potential of spectroscopic reflectance measurements (450 to 2450 nm) for tree species discrimination. We assess within- and among-species spectral variability and perform a feature selection procedure to identify wavebands in which the species most differ from each other. We assess the discriminative power of these wavebands by calculating a separability index and then classifying the species. Finally, leaf chemical and structural parameters of each species are retrieved by inversion of the leaf optical model PROSPECT-5. Among-species spectral variability is almost five times greater than within-species spectral variability. The feature selection procedure reveals that wavebands, where species most differ, are located at the visible, red edge, and shortwave infrared regions. Classification of the species using these wavebands reaches 96% overall accuracy. Leaf chemical and structural properties retrieve by model inversion show that differences in leaf pigment concentrations and leaf internal structure are the most important parameters controlling the spectral variability of species. These parameters also contribute to the variation in red edge position among species. © *2013 Society of Photo-Optical Instrumentation Engineers (SPIE)* [DOI: 10.1117/1.JRS.7.073502]

Keywords: species discrimination; tropical forest; Atlantic Forest; spectroscopy; PROSPECT-5.

Paper 13224 received Jun. 25, 2013; revised manuscript received Aug. 27, 2013; accepted for publication Sep. 10, 2013; published online Oct. 4, 2013.

1 Introduction

Management and conservation efforts of tropical forests require frequent floristic assessments to yield knowledge on species numbers and distribution. Such data are usually obtained by expensive and time-consuming field surveys, which make the development of alternative methods a promising research topic. Remote sensing can provide information about species richness over large areas at a low cost. Particularly, hyperspectral sensors have the capacity to slice the electromagnetic spectrum into hundreds of narrow spectral bands, enabling the detection of unique spectral signatures.[1] At the leaf-level, some studies successfully identified tree species with the hyperspectral data.[2–4] Within the scope of large-scale applications, hyperspectral imaging, also known as imaging spectroscopy, has also been used to map floristic composition in tropical forest sites.[1,5–8] This opened a new opportunity to monitor tropical species composition and, consequently, improve the understanding of anthropogenic impacts, such as land use and climate change, in forest ecosystems. Moreover, floristic studies by remote sensing can become a feasible way to assess species richness in areas of difficult access, where traditional field surveys are financially and operationally prohibitive.

0091-3286/2013/$25.00 © 2013 SPIE

Downloaded From: http://remotesensing.spiedigitallibrary.org/ on 12/06/2013 Terms of Use: http://spiedl.org/terms

However, species discrimination using a high spectral resolution remote sensing is not a trivial task. The spectral response of plants is governed by a relatively small number of physical parameters, which causes similarities among species.[9,10] In high-diversity forests, the precept for species recognition is that among-species spectral variability should exceed within-species spectral variability. Such assessment is crucial across a range of forest ecosystems to provide the basis for species discrimination with the hyperspectral data, yet few studies have dealt with the spectral variation of tree species. Perhaps, the most important contribution was made by Castro-Esau et al.[3] who performed an analysis of the spectral variability of >50 tropical dry forest trees and assessed its impact on species discrimination. In more recent years, Féret and Asner[11] provided a study of the variability in leaf optical properties of Hawaiian forest species. Although other examples of studies involving leaf optical properties of tropical trees could be quoted (e.g., Refs. 12–14), little is known about the spectral variability of Atlantic Forest (AF) tree species. Considered as a biodiversity hotspot for conservation priorities,[15] the AF still harbors an impressive number of endemic species and high biodiversity,[16] despite the exceptional loss of habitat.[17]

With the tropical tree species recognition using a hyperspectral data in a stage of increasing development, we believe it is valuable to provide an analysis of the spectral variability of AF tree species. Therefore, the main objectives of this article are to provide a practical understanding of the main sources of variability in leaf spectral signatures of AF tree species and to evaluate the potential of spectroscopy measurements for species discrimination. We investigated within- and among-species spectral variability of 315 leaf samples of 21 different trees. By a feature selection procedure, we identified the wavebands in which the species most differ. Then, a randomization procedure was performed to test if the differences among species means is or is not likely to have arisen by chance. Afterwards, aiming to quantify the spectral variation, we calculated a separability index for each of the wavebands where species most differ from each other. To assess the discriminative power of these wavebands, we carried out a supervised classification of the species. Finally, we performed simulations using the PROSPECT-5 model[18] to estimate leaf chemical and structural parameters.

2 Materials and Methods

2.1 *Location and Data Acquisition*

For this study, spectroscopy measurements were collected from leaves of seven AF tree species from a forested area located on the surroundings of Porto Alegre city, in southern Brazil (30°04′27′′S, 51°06′51′′W). A Plant Probe accessory, combined with the Leaf Clip assembly [Analytical Spectral Devices (ASD), Inc., Boulder, Colorado], coupled in the high-resolution spectroradiometer ASD/FieldSpec®3, was used to measure the reflectance of species leaves. The ASD/FieldSpec®3 instrument consists of three spectrometers. The first one covers the visible (VIS, 350 to 700 nm) and near-infrared (NIR, 701 to 1000 nm) regions of the electromagnetic spectrum and has a spectral resolution of 3 nm. The second and third spectrometers have a spectral resolution of 10 nm and cover the shortwave infrared (SWIR) region (1001 to 2500 nm). The Leaf Clip assembly is designed for use with the Plant Probe accessory, which has an integrated halogen bulb that emits radiation over the 350- to 2500-nm spectral range. Its design minimizes measurement errors associated with the stray light. Leaf Clip includes a gripping system for holding the target sample in place without inflicting damage to the leaf. It also has a two-sided rotating head (2 cm in diameter) that allows both bidirectional reflectance and transmittance measurements.[19] Figure 1 illustrates how leaf samples were spectrally measured using Plant Probe + Leaf Clip assembly.

Full sunlight leaves were detached from branches of AF tree species and immediately taken to the laboratory of spectroradiometry of the Federal University of Rio Grande do Sul (UFRGS). Table 1 shows the species names as well as the number of trees and leaves per tree sampled. The latter equaled 15 to ensure a representative sample size.[20] Leaves were detached and measured separately for each tree in order to preserve their physical and chemical characteristics. A reflectance standard (Spectralon, Labsphere Inc., Durham, New Hampshire) was used to calibrate the instrument for dark current and stray light and calculate the reflectance factor of the samples. In

Downloaded From: http://remotesensing.spiedigitallibrary.org/ on 12/06/2013 Terms of Use: http://spiedl.org/terms

Fig. 1 Leaf reflectance measurement using Plant Probe + Leaf Clip assembly. (Source: ASD, 2004.)

Table 1 Species names, number of trees, and number of leaves per tree sampled for reflectance measurements.

Species names	No. of trees sampled	No. of leaves per tree sampled
Psidium araca (PA)	3	15
Schinus terebinthifolius (ST)	3	15
Ocotea spixiana (OS)	3	15
Tabebuia impetiginosa (TI)	3	15
Ceiba speciosa (CS)	3	15
Bauhinia forficata (BF)	3	15
Eugenia uniflora (EU)	3	15

this study, the following spectral regions will be considered: VIS (400 to 700 nm), NIR (701 to 1300 nm), and SWIR (1301 to 2450 nm).

2.2 *Spectral Variability*

Aiming to assess within- and among-species spectral variability, we computed the metric D proposed by Price,[10] which is calculated as follows:

$$D = \left\{ \frac{1}{\lambda_b - \lambda_a} \int_{\lambda_a}^{\lambda_b} [S_1(\lambda) - S_2(\lambda)] d^2 \lambda \right\}^{1/2}, \tag{1}$$

where D corresponds to the root mean square difference between a pair of spectra (S_1 and S_2), averaged over the spectral interval (λ_a to λ_b). The spectral interval used to calculate this metric was 450 to 2450 nm. Although the ASD/FieldSpec®3 spectroradiometer engine with the spectral range from 350 to 2500 nm, the initial (below 450 nm) and final (after 2450 nm) wavebands presented noisy values and should be discarded.

D was calculated at the following levels for leaf spectra:

1. Within-tree: Multiple leaves were sampled per tree of each species (Table 1), D was computed for all pairwise combinations. Note that the total number of pairwise combinations was calculated as $n[(n-1)/2]$ and equaled 105, with n being the number of leaves.
2. Among-trees and within-species: Multiple trees of the same species were sampled (Table 1) and leaf spectral responses of each tree were averaged. D was computed for all pairwise combinations (i.e., three).

Downloaded From: http://remotesensing.spiedigitallibrary.org/ on 12/06/2013 Terms of Use: http://spiedl.org/terms

3. Among-species: Averaged spectra per species were calculated and D was computed for 21 pairwise combinations.

Finally, Wilcoxon rank sum test was performed to determine whether within-species and among-species spectral variability were statistically significantly different.

2.3 *Statistical Procedures*

Aiming to assess the spectral variability of species, we were interested in identifying regions of the electromagnetic spectrum in which the species most differ from each other. For this purpose, we first conducted a one-way analysis of variance (ANOVA) followed by the post-hoc Tukey Honestly Significance Difference (HSD) test across each waveband, in order to verify differences among species means. Second, a randomization test was performed to provide information whether the pattern observed in the data (statistically significantly different pairs) is likely, or not, to have arisen by chance. Finally, we estimated the spectral separability between species by the Jeffries-Matusita (JM) distance and performed a classification of the species using linear discriminant analysis (LDA). These methods have proved to be universally superior for the optimal feature selection[21] and have been successfully used for spectral discrimination of plant species.[22–24] Prior to performing the statistical tests, normality and homoscedasticity (homogeneity of variances) of the reflectance values across each waveband were verified.

2.3.1 *Feature selection*

One-way ANOVA test was used to verify the statistical difference between species means in each waveband. The ANOVA tested the following hypothesis:

$$H_0 = \mu_1 = \mu_2 = \cdots = \mu_n, \tag{2}$$

$$H_1 = \text{Not all}\, \mu_n(i)\, \text{are equal}, \tag{3}$$

where μ_n represents the mean reflectance of the n'th species $(n = 1, 2, \ldots, 7)$ and i denotes the waveband. Rejection of the null hypothesis (H_0) indicated the wavebands, at a 99% (p-value <0.01) confidence level, in which the species differ statistically. H_0 rejection was followed by pairwise multiple comparisons with the post-hoc Tukey HSD test. The total number of pair combinations was calculated as $n[(n-1)/2]$ and equaled 21, where n is the number of species. By counting the number of pairs that is statistically significantly different on each waveband, it is possible to identify the spectral regions where the species most differ. Only the wavebands with 19 or more statistically significantly different pairs were retained for further use. This number was chosen because it represents >90% of total pairwise combinations, evidencing the wavebands that may have high discriminative power.

2.3.2 *Randomization test*

With the randomization procedure, we tested if the differences among species means it is or is not likely to have arisen by chance.[25] The procedure of randomization was performed according to Manly[25] as follows. First, the F statistic was chosen to measure the extent to which the data show the pattern in question. Second, F-values were estimated at each waveband for the observed reflectance measurements. Then, these values were randomly reallocated 4999 times while holding the categorical variable (tree species), and the F statistic was recomputed for each randomization.

According to Manly,[25] the results from randomization tests can be interpreted in the same way as for conventional tests of significance. However, the level of significance should be interpreted as a measure of the strength of evidence against the null hypothesis (equal species means). In our case, this measure can be estimated by the number of F-values that was lower than the observed F-values.

Downloaded From: http://remotesensing.spiedigitallibrary.org/ on 12/06/2013 Terms of Use: http://spiedl.org/terms

2.3.3 *Spectral separability*

Aiming to estimate the spectral separability of species at the wavebands previously identified, we calculated the Jeffries-Matusita (JM) distance. According to Richards and Jia,[26] JM distance is calculated using Eq. (4):

$$\mathrm{JM}_{ij} = 2(1 - e^{-B}), \tag{4}$$

in which

$$B = \frac{1}{8}(m_i - m_j)^T \left(\frac{\sum i + \sum j}{2}\right)^{-1} (m_i - m_j) + \frac{1}{2} \ln \left[\frac{\left|\left(\sum i + \sum j\right)/2\right|}{\left|\sum i\right|^{1/2} \left|\sum j\right|^{1/2}}\right], \tag{5}$$

which is known as Bhattacharyya distance,[27] where i and j are the two species being compared, $\sum_i$ = covariance matrix of i species, $\sum_j$ = covariance matrix of j species, m_i = mean vector of i, m_j = mean vector of j, T = transposition function, ln = natural logarithm, $|\sum_i|$ = determinant of $\sum_i$, and $|\sum_i|$ = determinant of $\sum_j$. The calculation of $\sum_i$ and $\sum_j$ as well as m_i and m_j was possible for each selected waveband because 45 samples per species were obtained (Table 1). JM distance values vary between 0 and 2, with higher values indicating the total separability of the species pairs in the wavebands being used.[26] Processing procedures until here were performed in the R environment.[28]

2.3.4 *Classification*

JM distance was calculated to quantify the spectral separability of species at the wavebands with higher counts of statistically different pairs. To test the relevance of these wavebands for species discrimination, LDA was performed. This pattern recognition technique is used to separate two or more classes of objects with a linear combination of features.[29] LDA has proved to have a good performance for the classification of tree species using the hyperspectral remotely sensed data.[1,7,8] Here, a cross-validated LDA classifier with 10-folds was created using the MATLAB® Statistics Toolbox. First, the training sample was randomly divided into 10 subsamples of roughly equal size. Then, a leave-one-out approach was used in the cross-validation process to assess the predictive power of the model. In this approach, one subsample is removed and the model is trained with the remaining ones. The removed sample is then classified by the trained model. After repeating this process 10 times (folds) the average confusion matrix was computed as well as user, producer, and overall accuracies.

2.4 *PROSPECT-5 Simulations*

PROSPECT[9] has become the most important model to simulate leaf reflectance and transmittance over the optical domain (400 to 2500 nm).[30] This model has undergone gradual improvements and is currently in its fifth version.[18] With a set of input variables [leaf structure parameter (N), chlorophyll $a + b(C_{ab})$, carotenoids (C_{ar}), equivalent water thickness (C_w), and dry matter content (C_m)], PROSPECT-5 simulates leaf directional-hemispherical reflectance and transmittance over the 400- to 2500-nm spectral range. The N parameter is used to consider differences in leaf anatomy among species.[9] As we did not perform any chemical analysis for the species studied, the mentioned set of parameters was not available. Therefore, it was retrieved by inversion of the PROSPECT-5. For this purpose, a MATLAB® code, freely available at http://teledetection.ipgp.jussieu.fr/prosail/, was used. Inversion of the PROSPECT-5 is performed by finding the best set of parameters (θ) that minimizes the merit function using Eq. (6):

$$G(\theta) = \sum_{\lambda_{\min}}^{\lambda_{\max}} \{[R_{\mathrm{mes}}(\lambda) - R_{\mathrm{sim}}(\lambda, \theta)]^2 + [T_{\mathrm{mes}}(\lambda) - T_{\mathrm{sim}}(\lambda, \theta)]^2\}, \tag{6}$$

where R_{mes} and T_{mes} are the measured reflectance and transmittance and R_{sim} and T_{sim} are the simulated reflectance and transmittance. The Nelder–Mead Simplex method[31] with bound

Downloaded From: http://remotesensing.spiedigitallibrary.org/ on 12/06/2013 Terms of Use: http://spiedl.org/terms

constraints was applied to minimize $G(\theta)$. In this study, we considered only the simulated reflectance.

3 Results and Discussion

3.1 *Spectral Variability*

Spectral variability is a key factor in discriminating tree species with the hyperspectral data. In this study, assessment of within- and among-species variability was possible because leaves of same- and different-species trees were measured. Within- and among-species variability, estimated using Eq. (1), differed statistically (Wilcoxon rank sum test p-value <0.01). Spectral amplitude (D) values showed an increasing trend of within-to-among species (Fig. 2). This agrees with Féret and Asner,[11] who explored the spectral variability of Hawaiian tropical trees for classification purposes. Among-species D was almost five times greater than within-species D. Given the magnitude of this difference, AF tree species could be discriminated using the hyperspectral data.

3.2 *Statistical Analysis*

Differences in leaf spectra were verified by one-way ANOVA followed by Tukey HSD post-hoc test. One-way ANOVA results indicated that species are likely to be spectrally separable (p-value < 0.01) at 1488 wavebands on the reflectance spectra (74.4% of a total 2000). Tukey HSD post-hoc test resulted in 21 possible pairwise combinations for the number of species sampled. A total of 63 bands presented at least 19 statistically significantly different pairs (gray areas in Fig. 3). Spectral variability of species is concentrated at these wavelengths, which are located at the VIS (450 to 700 nm), red edge (680 to 760 nm), and SWIR (1001 to 2450 nm) regions (Fig. 3). Most notably, several wavebands were selected around the green peak (550 nm), which is formed due to the strong absorption of leaf pigments. It is worth noting that chlorophylls (chlorophyll a and b) and carotenoids absorb light in the vicinity of 445 and 645 nm[32] and 350 to 450 nm,[33] respectively. This is the evidence that species have varied concentrations of such pigments.

Some wavebands were also selected at the beginning of red edge (680 to 760 nm) (Fig. 2). At this region, an abrupt variation in leaf spectra occurs as a result of strong chlorophyll absorption at red (650 to 700 nm) and high reflectance at NIR due to multiple-scattering at the air-cell

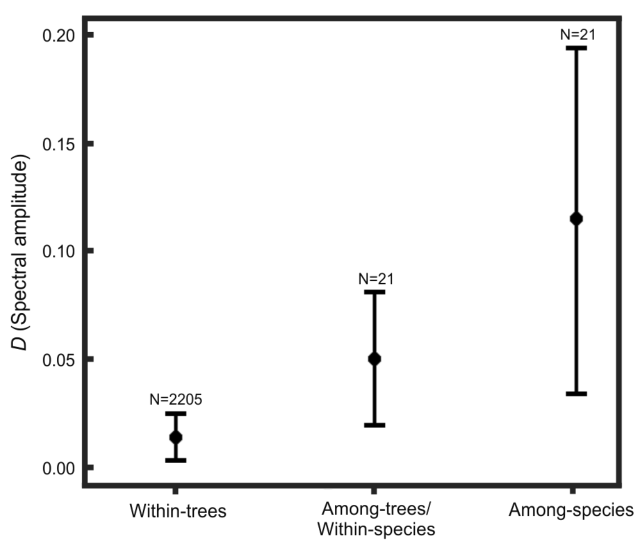

Fig. 2 Mean spectral amplitude (D) (± 1 standard deviation) of leaf reflectance spectra of Brazilian Atlantic Forest (AF) tree species. Number of samples to calculate each mean is indicated.

Downloaded From: http://remotesensing.spiedigitallibrary.org/ on 12/06/2013 Terms of Use: http://spiedl.org/terms

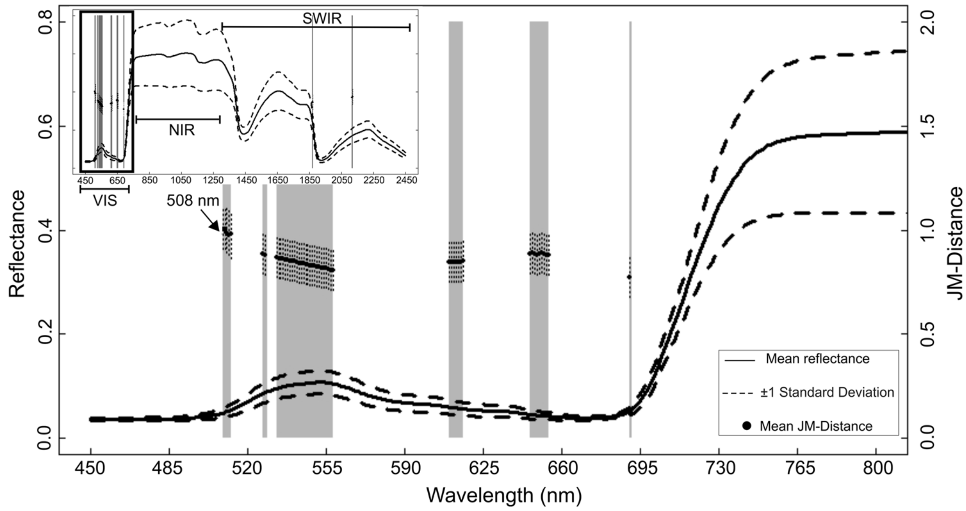

Fig. 3 Leaf reflectance measurements of Brazilian AF tree species. Gray areas represent the wavebands where the species most differ from each other. Mean Jeffries-Matusita (JM)-distance values are inserted to indicate the spectral separability among species at these wavebands. The waveband that achieved the highest JM-distance value is indicated.

interfaces in the internal leaf tissue.[34] As a result, the red edge position, i.e., point of maximum slope in the vegetation spectra, has a relationship with the leaf chlorophyll concentration[32] and leaf scattering properties.[34] Therefore, the red edge position has been explored in several vegetation studies.[35–37] Here, just a few wavebands were selected at the red edge, which may suggest this region did not have a significant contribution on the species discrimination. However, the separability threshold applied (19 or more statistically significantly different pairs) was quite restrictive. It is possible that wavebands with 17 or 18 statistically different pairs could also provide useful information to separate the species.

In order to quantify the spectral variation at the selected wavebands, the JM-distance [Eq. (4)] between each species pairs was calculated. Figure 3 shows mean JM-distance values as black dots with respective ± 1 standard deviation bars. For reflectance measurements, higher separability values are found at 508- to 515-nm interval (Fig. 3), in which the waveband located at 508 nm achieved the highest value.

Differences in leaf pigments demonstrated to be a very important factor on the spectral variability of species, which led to variations at the red edge position among them (Table 3). This result is consistent with Cochrane[2] and Rivard et al.[20] who also showed that the red edge position is relevant for discrimination of tropical forest trees. Conversely, our findings partially disagree with Clark and Roberts,[7] who found that the most important reflectance bands for classifying leaves are located at NIR and SWIR regions instead of VIS and NIR regions as we propose here. This difference may be due to the gap in time between leaf spectra acquisitions. Clark and Roberts[7] measured bidirectional reflectance of leaves 12 h from the time of collection at the field site, which considerably affected the leaf moisture content and, consequently, SWIR reflectance. In our work, leaves were measured immediately after being detached from trees and variation in leaf moisture content was low (Table 3). Nevertheless, some wavebands were selected at the SWIR around 1850 and 2100 nm (Fig. 3). Structural constituents, such as lignin and cellulose, are obscured due to the strong water absorption in this spectral region.[38] Species with leathery leaves can significantly influence SWIR reflectance which was the case of *Psidium araca* (PA). PA reached the highest dry matter content (C_w) value and also the highest leaf structure parameter (N) (Table 3), both of them retrieved by inversion of the PROSPECT-5 model.

To ensure that differences in leaf spectra have not arisen by chance, we performed a randomization test. The observed values were found after 99% of the randomizations (Fig. 4). This means that <1% of the F-values calculated after randomization were greater than the observed F-value, which provides very strong evidence against the null hypothesis [equal species means, Eq. (2)].

Downloaded From: http://remotesensing.spiedigitallibrary.org/ on 12/06/2013 Terms of Use: http://spiedl.org/terms

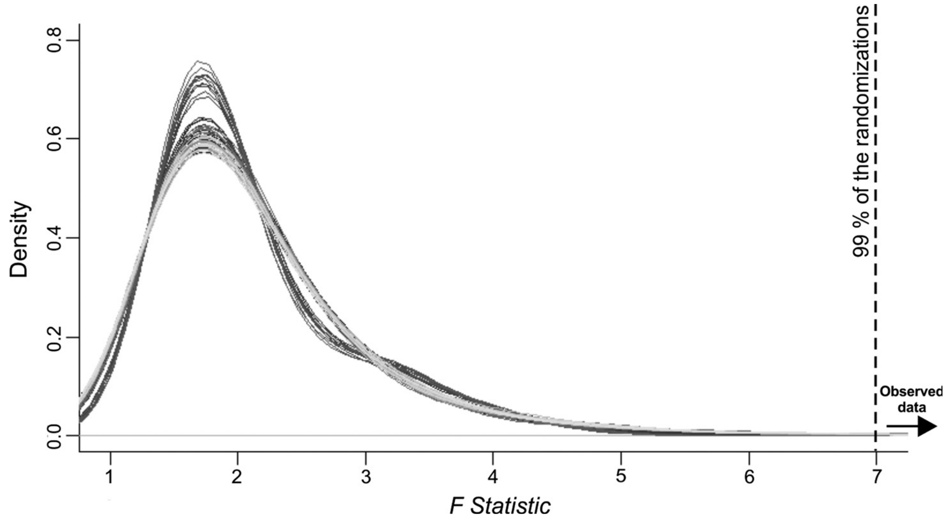

Fig. 4 Density histogram of F-values obtained after randomly reallocate 4999 times the reflectance values of the wavebands in which the species most differ (see Fig. 3), each gray line represents a waveband. The observed F-values are found after the threshold that contains 99% of the F-values calculated after randomization.

Finally, LDA was used to classify the species based on the spectral behavior at the wavebands identified by the feature selection procedure. Results of the 10-fold leave-one-out cross-validation are shown in Table 2. Overall accuracy was high (96.2%) confirming that wavebands selected are adequate for multiple species classification of the data set. The highest confusion rates were reported between OS/EU and TI/CS, which indicated that these species have similar spectral responses. In general, most of the trees were correctly classified, reaching even 100% accuracy.

3.3 *Leaf Chemical and Structural Properties*

In order to corroborate the results previously presented, leaf chemical and structural parameters of species were retrieved by inversion of the PROSPECT-5 model. This inversion is based solely

Table 2 Confusion matrix resulted from linear discriminant analysis using the wavebands in which the species most differ from each other. The diagonal elements are the counts of the correct predictions.

	PA	ST	OS	TI	CS	BF	EU	Row total	User accuracy (%)
PA	45	0	0	0	0	0	0	45	100
ST	0	43	0	1	0	1	0	45	96
OS	0	0	43	0	0	0	2	45	96
TI	0	0	0	43	2	0	0	45	96
CS	0	0	0	1	43	1	0	45	96
BF	0	1	0	0	0	44	0	45	98
EU	0	1	2	0	0	0	42	45	93
Column total	45	45	45	45	45	46	44	303	
Producer accuracy (%)	100	96	96	96	96	96	95		
Overall accuracy (%) $= 96.2$									

Downloaded From: http://remotesensing.spiedigitallibrary.org/ on 12/06/2013 Terms of Use: http://spiedl.org/terms

Table 3 Leaf chemical and structural parameters obtained by inversion of the PROSPECT-5 leaf optical model and red edge position of species.

Species names	N	C_{ab} (μg/cm^2)	C_{ar} (μg/cm^2)	C_w (g/cm^2)	C_m (g/cm^2)	Red edge position (nm)
PA	2.66	58.31	12.76	0.024	0.011	709
ST	1.88	50.76	10.78	0.019	0.008	715
OS	1.93	57.98	13.73	0.013	0.007	724
TI	1.66	52.00	13.00	0.008	0.006	719
CS	1.48	50.00	12.00	0.009	0.005	713
BF	1.64	42.80	9.50	0.009	0.003	722
EU	1.86	77.58	17.17	0.010	0.008	705

Note: N = leaf structure parameter; C_{ab} = chlorophyll content $(a + b)$; C_{ar} = carotenoids content; C_w = equivalent water thickness; C_m = dry matter content.

on species spectra and is considered as a feasible way to estimate biophysical parameters of vegetation.[16] Simulated reflectance values were very similar to the measured ones, as shown in Fig. 5, and high-correlation coefficients were achieved. The retrieved variables as well as red edge positions (wavebands with the maximum slope in vegetation spectra) are presented in Table 3.

Remarkably, chlorophyll $a + b\,(C_{ab})$ concentration varied from 77.58 μg/cm^2 in *Eugenia uniflora* (EU) to 42.80 μg/cm^2 in *Bauhinia forficata* (BF), or nearly double. Carotenoids (C_{ar}) concentrations were not as varied as C_{ab}, with the exception of EU. Equivalent water thickness (C_w) parameters were similar among species, except for species with the high dry matter content (C_m) such as PA. Moreover, similar C_m values were obtained because measurements were performed immediately after detaching the leaves from tree branches. Finally, considerable variation was observed at the leaf structure parameter (N), evidencing that the model accounted for differences in leaf anatomy among species. As noted by Féret and Asner[11] correct values of N parameter are crucial to obtain an accurate leaf spectrum model.

The inversion of the PROSPECT-5 model provided favorable results corroborating evidences that leaf pigments and red edge position determine the spectral variability of AF tree species. Consequently, it was proved that the spectral regions best suited to discriminate the species studied are located at VIS and NIR regions of the electromagnetic spectrum. Although, these findings are closely related to the database used in this work, they are important contributions to the progress of hyperspectral discrimination of tree species. Especially for the Brazilian AF, in which investigations such as those carried out in this work have been poorly reported in the literature.

4 Conclusions

In this study, we analyzed the spectral variability of AF tree species from full-range (450 to 2450 nm) leaf spectroscopy data. We focused on 21 trees of seven important species from a site in the south of Brazil. Our study showed that the spectral diversity of species is mostly determined by leaf pigment concentrations, red edge position, and SWIR reflectance. Using the spectral information presented in the wavebands located at these regions, high overall accuracy was reached (96.2%). It is of value to note that this accuracy rate is intrinsic to the data set and to the methodology employed in this study. Moreover, among-species spectral variability was considerably higher than within-species variability. These findings are important contributions for hyperspectral research on tropical species discrimination for two main reasons. First, assessment of within- and among-species spectral variability is a prerequisite for species discrimination. Second, optimal feature selection is a crucial task in the hyperspectral data processing. Thus, identification of separable regions along with the optical domain depends

Downloaded From: http://remotesensing.spiedigitallibrary.org/ on 12/06/2013 Terms of Use: http://spiedl.org/terms

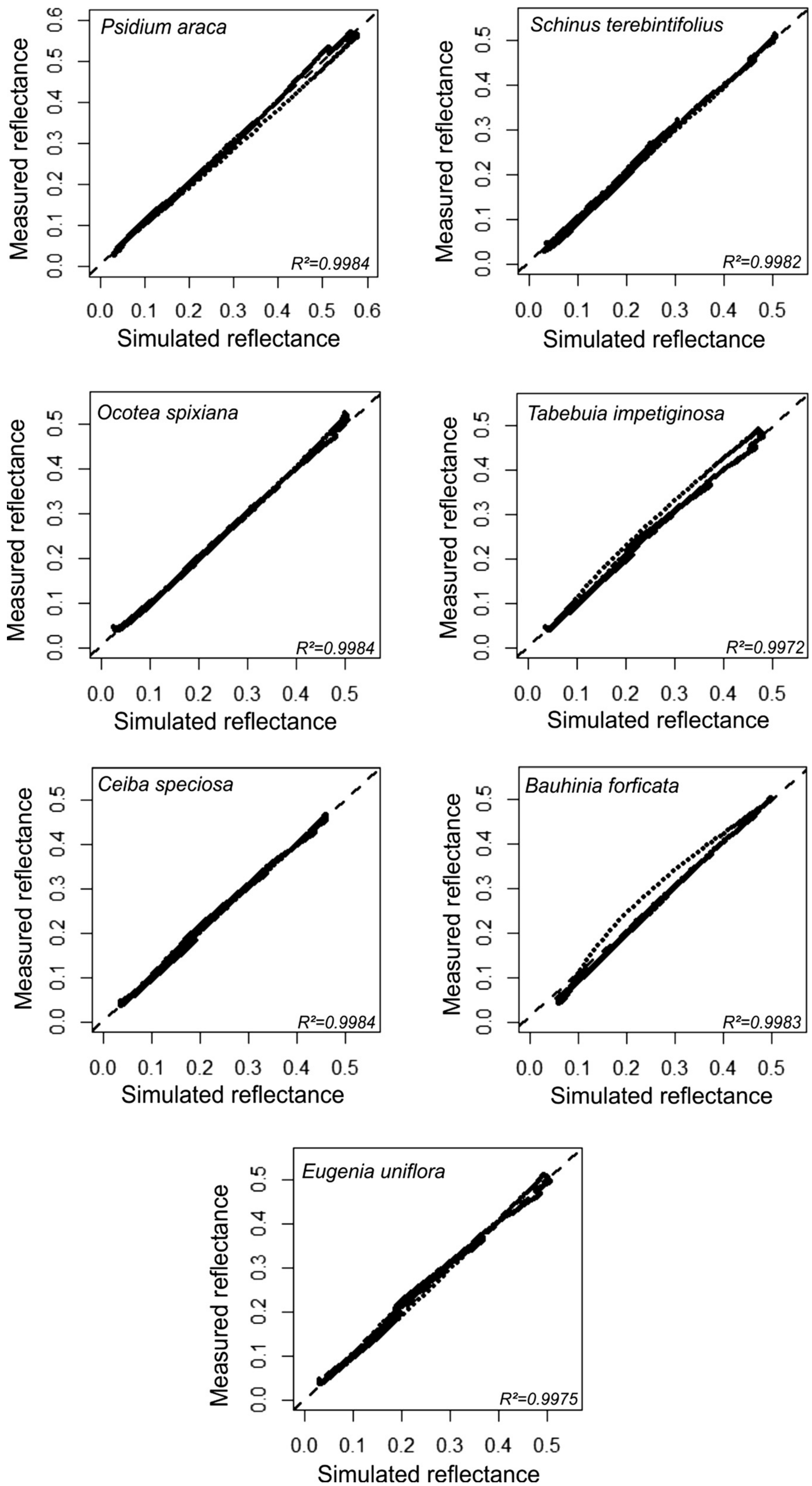

Fig. 5 Relationships between measured and modeled reflectance of species. Dashed lines represent perfect correlation between the variables. The R^2 values and species names are shown in each graphic.

Downloaded From: http://remotesensing.spiedigitallibrary.org/ on 12/06/2013 Terms of Use: http://spiedl.org/terms

on an initial attempt to spectrally discriminate plant species in the AF Biome. Nevertheless, others' investigations such as this must be carried out with more species and at different regions to account for the high diversity of AF.

The methodological approach developed in this article proved to be useful to assess the spectral variability of species in an efficient way. Most notably, the inversion of the PROSPECT-5 model provided accurate estimations of leaf spectra ($\bar{r}^2 = 0.99$), although no chemical data were available. Furthermore, a calculation of JM distance across each spectrally separable waveband is an innovative approach that, coupled with the LDA classification, permitted quantification of the discriminative power of these bands (Fig. 3).

To conclude the evidence that spectral signatures linked to leaf chemical properties are unique for tropical tree species[5] motivates the development of approaches that might map canopy species over large areas. Additionally, the possibility of mapping canopy chemicals with the hyperspectral data[39] is a substantial advance in vegetation monitoring. However, analytical methods to achieve these goals are just beginning to appear and much more research is needed. Recently, acquisitions of high-resolution hyperspectral imagery over AF areas have motivated even more research related to canopy chemistry and species mapping in this Biome.

Acknowledgments

We thank the Foundation for Research Support of the State of Rio Grande do Sul (FAPERGS) for supporting this work and two anonymous reviewers for their valuable comments on this manuscript.

References

1. M. Clark, D. Roberts, and D. Clark, "Hyperspectral discrimination of tropical rain forest tree species at leaf to crown scales," *Remote Sens. Environ.* **96**(3–4), 375–398 (2005), http://dx.doi.org/10.1016/j.rse.2005.03.009.
2. M. A. Cochrane, "Using vegetation reflectance variability for species level classification of hyperspectral data," *Int. J. Remote Sens.* **21**(10), 2075–2087 (2000), http://dx.doi.org/10.1080/014311600050021303.
3. K. L. Castro-Esau et al., "Variability in leaf optical properties of mesoamerican trees and the potential for species classification," *Am. J. Bot.* **93**(4), 517–530 (2006), http://dx.doi.org/10.3732/ajb.93.4.517.
4. R. Pu, "Broadleaf species recognition with in situ hyperspectral data," *Int. J. Remote Sens.* **30**(11), 2759–2779 (2009), http://dx.doi.org/10.1080/01431160802555820.
5. G. P. Asner and R. E. Martin, "Airborne spectranomics: mapping canopy chemical and taxonomic diversity in tropical forests," *Front. Ecol. Environ.* **7**(5), 269–276 (2009), http://dx.doi.org/10.1890/070152.
6. M. Papeş et al., "Using hyperspectral satellite imagery for regional inventories: a test with tropical emergent trees in the Amazon Basin," *J. Veg. Sci.* **21**(2), 342–354 (2010), http://dx.doi.org/10.1111/jvs.2010.21.issue-2.
7. M. L. Clark and D. Roberts, "Species-level differences in hyperspectral metrics among tropical rainforest trees as determined by a tree-based classifier," *Remote Sens.* **4**(12), 1820–1855 (2012), http://dx.doi.org/10.3390/rs4061820.
8. J.-B. Féret and G. P. Asner, "Tree species discrimination in tropical forests using airborne imaging spectroscopy," *IEEE Trans. Geosci. Remote Sens.* **51**(1), 73–84 (2013), http://dx.doi.org/10.1109/TGRS.2012.2199323.
9. S. Jacquemoud and F. Baret, "PROSPECT: a model of leaf optical properties spectra," *Remote Sens. Environ.* **34**(2), 75–91 (1990), http://dx.doi.org/10.1016/0034-4257(90)90100-Z.
10. J. C. Price, "How unique are spectral signatures?" *Remote Sens. Environ.* **49**(3), 181–186 (1994), http://dx.doi.org/10.1016/0034-4257(94)90013-2.
11. J. Féret and G. P. Asner, "Spectroscopic classification of tropical forest species using radiative transfer modeling," *Remote Sens. Environ.* **115**(9), 2415–2422 (2011), http://dx.doi.org/10.1016/j.rse.2011.05.004.
12. L. Poorter et al., "Leaf optical properties in Venezuelan cloud forest trees," *Tree Physiol.* **20**(8), 519–526 (2000), http://dx.doi.org/10.1093/treephys/20.8.519.

Downloaded From: http://remotesensing.spiedigitallibrary.org/ on 12/06/2013 Terms of Use: http://spiedl.org/terms

13. G. P. Asner et al., "Leaf chemical and spectral diversity in Australian tropical forests," *Ecol. Appl.* **19**(1), 236–253 (2009), http://dx.doi.org/10.1890/08-0023.1.
14. G. A. Sánchez-Azofeifa et al., "Differences in leaf traits, leaf internal structure, and spectral reflectance between two communities of lianas and trees: implications for remote sensing in tropical environments," *Remote Sens. Environ.* **113**(10), 2076–2088 (2009), http://dx.doi.org/10.1016/j.rse.2009.05.013.
15. N. Myers et al., "Biodiversity hotspots for conservation priorities," *Nature* **403**(6772), 853–858 (2000), http://dx.doi.org/10.1038/35002501.
16. R. A. Mittermeier, N. Myers, and G. P. E. Robles, *Hotspots*, Agrupación Sierra Madre, Mexico City (1999).
17. L. P. C. Morellato and C. F. B. Haddad, "Introduction: the Brazilian Atlantic Forest," *Biotropica* **32**(4b), 786–792 (2000), http://dx.doi.org/10.1646/0006-3606.
18. J.-B. Féret et al., "PROSPECT-4 and 5: advances in the leaf optical properties model separating photosynthetic pigments," *Remote Sens. Environ.* **112**(6), 3030–3043 (2008), http://dx.doi.org/10.1016/j.rse.2008.02.012.
19. Analytical Spectral Devices (ASD), "Leaf Clip Product Sheet," ASD Inc., http://www.asdi.com/products/accessories/contact-sampling-accessories/leaf-clip (28 February 2013).
20. B. Rivard et al., "Species classification of tropical tree leaf reflectance and dependence on selection of spectral bands," Chapter 6 in *Hyperspectral Remote Sensing of Tropical and Sub-Tropical Forests*, M.Kalácska and G. A. Sánchez-Azofeifa, Eds., pp. 261–296, CRC Press, Boca Raton, FL (2006).
21. Y. H. Yang, Y. Xiao, and M. R. Segal, "Identifying differentially expressed genes from microarray experiments via statistic synthesis," *Bioinformatics* **21**(7), 1084–1093 (2005), http://dx.doi.org/10.1093/bioinformatics/bti108.
22. C. Vaiphasa et al., "A hyperspectral band selector for plant species discrimination," *ISPRS J. Photogramm. Remote Sens.* **62**(3), 225–235 (2007), http://dx.doi.org/10.1016/j.isprsjprs.2007.05.006.
23. E. Adam and O. Mutanga, "Spectral discrimination of papyrus vegetation (Cyperus papyrus L.) in swamp wetlands using field spectrometry," *ISPRS J. Photogramm. Remote Sens.* **64**(6), 612–620 (2009), http://dx.doi.org/10.1016/j.isprsjprs.2009.04.004.
24. S. Ullah et al., "Identifying plant species using mid-wave infrared (2.5–6 μm) and thermal infrared (8–14 μm) emissivity spectra," *Remote Sens. Environ.* **118**(4), 95–102 (2012), http://dx.doi.org/10.1016/j.rse.2011.11.008.
25. B. Manly, *Randomization, Bootstrap and Monte Carlo Methods in Biology*, 2nd ed., Chapman & Hall, New York (1997).
26. J. A. Richards and X. Jia, *Remote Sensing Digital Image Analysis*, Springer Berlin Heidelberg, Berlin, Heidelberg (1999).
27. T. Kailath, "The divergence and Bhattacharyya distance measures in signal selection," *IEEE Trans. Commun. Technol.* **15**(1), 52–60 (1967), http://dx.doi.org/10.1109/TCOM.1967.1089532.
28. R Development Core Team, *R: A Language and Environment for Statistical Computing*, R Foundation for Statistical Computing, Vienna (2011).
29. S. Mika et al., "Fisher discriminant analysis with kernels," in *Proc. of the 1999 IEEE Signal Processing Society Workshop. Neural Networks for Signal Processing IX*, pp. 41–48, IEEE Signal Processing Society, Madison (1999), http://dx.doi.org/10.1109/NNSP.1999.788121.
30. S. Jacquemoud et al., "PROSPECT + SAIL models: a review of use for vegetation characterization," *Remote Sens. Environ.* **113**(Supplement 1), S56–S66 (2009), http://dx.doi.org/10.1016/j.rse.2008.01.026.
31. J. C. Lagarias et al., "Convergence properties of the Nelder-Mead simplex method in low dimensions," *SIAM J Optim.* **9**(1), 112–147 (1998), http://dx.doi.org/10.1137/S1052623496303470.
32. J. R. Thomas and H. W. Gausman, "Leaf reflectance vs. leaf chlorophyll and carotenoid concentrations for eight crops," *Agron. J.* **69**(5), 799–802 (1977), http://dx.doi.org/10.2134/agronj1977.00021962006900050017x.
33. G. A. Blackburn, "Hyperspectral remote sensing of plant pigments," *J. Exp. Bot.* **58**(4), 855–867 (2006), http://dx.doi.org/10.1093/jxb/erl123.

Downloaded From: http://remotesensing.spiedigitallibrary.org/ on 12/06/2013 Terms of Use: http://spiedl.org/terms

34. D. N. H. Holer, M. Dockray, and J. Barber, "The red edge of plant leaf reflectance," *Int. J. Remote Sens.* **4**(2), 273–288 (1983), http://dx.doi.org/10.1080/01431168308948546.
35. I. Filella and J. Peñuelas, "The red edge position and shape as indicators of plant chlorophyll content, biomass and hydric status," *Int. J. Remote Sens.* **15**(7), 1458–1470 (1994), http://dx.doi.org/10.1080/01431169408954177.
36. O. Mutanga and A. K. Skidmore, "Red edge shift and biochemical content in grass canopies," *ISPRS J. Photogramm. Remote Sens.* **62**(1), 34–42 (2007), http://dx.doi.org/10.1016/j.isprsjprs.2007.02.001.
37. I. D. Sanches et al., "Unravelling remote sensing signatures of plants contaminated with gasoline and diesel: an approach using the red edge spectral feature," *Environ. Pollut.* **174**, 16–27 (2013), http://dx.doi.org/10.1016/j.envpol.2012.10.029.
38. J. T. Woolley, "Reflectance and transmittance of light by leaves," *Plant Physiol.* **47**(5), 656–662 (1971), http://dx.doi.org/10.1104/pp.47.5.656.
39. K. M. Dahlin, G. P. Asner, and C. B. Field, "Environmental and community controls on plant canopy chemistry in a Mediterranean-type ecosystem," *Proc. Natl. Acad. Sci.* **110**(17), 1–6 (2013), http://dx.doi.org/10.1073/pnas.1215513110.

Matheus Pinheiro Ferreira received his BS degree in forest engineering from the Federal University of Paraná, Curitiba, Brazil, in 2010, and the MSc degree in remote sensing from the Brazilian National Institute for Space Research (INPE), São José dos Campos, Brazil in 2012. Currently, he is a PhD candidate in remote sensing at INPE, São José dos Campos, Brazil. His scientific research focuses on hyperspectral remote sensing of vegetation, including species identification, canopy chemistry, image processing and field spectroscopy.

Silvia Beatriz Alves Rolim is a geologist with MSc degree in remote sensing (National Institute for Space Research, SP) and PhD degree in geosciences State University of Campinas (UNICAMP, SP). She is an associated professor of the Federal University of Rio Grande do Sul [Federal University of Rio Grande do Su (UFRGS) —Brazil]; a researcher of the State Center for Research on Remote Sensing and Meteorology; and a chamber of postgraduate programs of UFRGS. Her research lines include radiative transfer processes and optical radiometry focused on geosciences.

Yosio Edemir Shimabukuro received his BS degree in forestry engineering from the Federal Rural University of Rio de Janeiro (UFRRJ), Seropédica, Brazil, in 1972 and the MS and PhD degrees in remote sensing from the Brazilian Institute for Space Research (INPE), São José dos Campos, Brazil, in 1977 and 1987, respectively. From January 1992 to March 1994, he was a visiting scientist with the Biospheric Sciences Branch, NASA Goddard Space Flight Center, Greenbelt, MD. Since 1973, he has been with INPE, studying satellite and ground-based remote sensing data for studying vegetation cover. He has been applying remote sensing and geographic information system techniques and models for environmental change detection over different biomes in Brazil.

Atilio Efrain Bica Grondona received the BA degree in mathematics from the Pontifical Catholic University of Rio Grande do Sul (PUC-RS), Porto Alegre, Brazil in 2004, and the MSc degree in remote sensing from Federal University of Rio Grande do Sul (UFRGS), Porto Alegre, Brazil, in 2011. Currently, he is a PhD candidate in remote sensing at UFRGS. His scientific research focuses on pattern recognition and temperature/emissivity separation algorithms in thermal infrared data.

Downloaded From: http://remotesensing.spiedigitallibrary.org/ on 12/06/2013 Terms of Use: http://spiedl.org/terms